IEEE Photonics Journal
An IEEE Photonics Society Publication

Invited Paper

Tunable Delay Lines in Silicon Photonics: Coupled Resonators and Photonic Crystals, a Comparison

Volume 2, Number 2, April 2010

A. Melloni
A. Canciamilla
C. Ferrari
F. Morichetti
L. O'Faolain
T. F. Krauss
R. De La Rue
A. Samarelli
M. Sorel

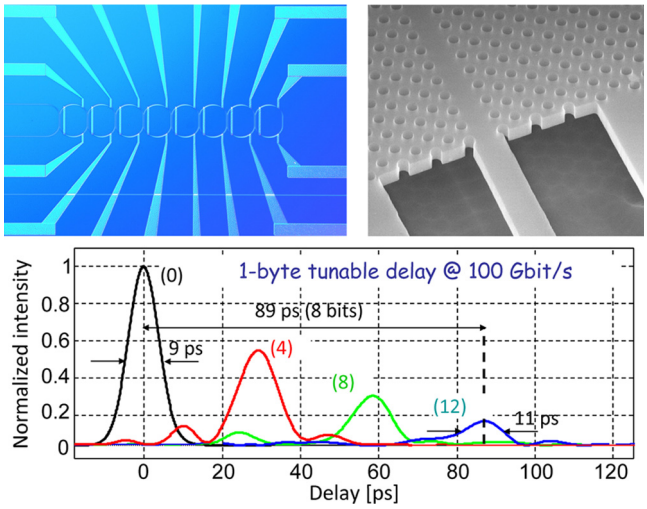

DOI: 10.1109/JPHOT.2010.2044989
1943-0655/$26.00 ©2010 IEEE

Tunable Delay Lines in Silicon Photonics: Coupled Resonators and Photonic Crystals, a Comparison

A. Melloni,[1] A. Canciamilla,[1] C. Ferrari,[1] F. Morichetti,[1,2] L. O'Faolain,[3] T. F. Krauss,[3] R. De La Rue,[4] A. Samarelli,[4] and M. Sorel[4]

(Invited Paper)

[1]Dipartimento di Elettronica e Informazione, Politecnico di Milano, 20133 Milano, Italy
[2]Fondazione Politecnico di Milano, 20133 Milano, Italy
[3]School of Physics and Astronomy, University of St. Andrews, KY16 9SS St. Andrews, U.K.
[4]Department of Electronics and Electrical Engineering, University of Glasgow, G12 8LP Glasgow, U.K.

DOI: 10.1109/JPHOT.2010.2044989

Manuscript received February 10, 2010; revised March 1, 2010. First published Online March 3, 2010. Current version published March 26, 2010. This work was supported in part by EU-FP6 FET project BSPLASH. Corresponding author: A. Melloni (e-mail: melloni@elet.polimi.it).

Abstract: In this paper, we report a direct comparison between coupled resonator optical waveguides (CROWs) and photonic crystal waveguides (PhCWs), which have both been exploited as tunable delay lines. The two structures were fabricated on the same silicon-on-insulator (SOI) technological platform, with the same fabrication facilities and evaluated under the same signal bit-rate conditions. We compare the frequency- and time-domain response of the two structures; the physical mechanism underlying the tuning of the delay; the main limits induced by loss, dispersion, and structural disorder; and the impact of CROW and PhCW tunable delay lines on the transmission of data stream intensity and phase modulated up to 100 Gb/s. The main result of this study is that, in the considered domain of applications, CROWs and PhCWs behave much more similarly than one would expect. At data rates around 100 Gb/s, CROWs and PhCWs can be placed in competition. Lower data rates, where longer absolute delays are required and propagation loss becomes a critical issue, are the preferred domain of CROWs fabricated with large ring resonators, while at data rates in the terabit range, PhCWs remain the leading technology.

Index Terms: Slow light, delay lines, coupled resonators, rings, silicon photonics, photonic crystals, differential quadrature phase shift keying (DQPSK).

1. Introduction

Slow-light optical devices have been intensively studied in the last decade because of their unique properties for enhancing light-matter interactions and handling the flow of light. Among the variety of features connected to the concept of slow light, the ability of controlling the optical group velocity and/or the group delay of the light can find applications in the realization of variable delay lines and devices for optical storage and buffering [1].

In passive integrated devices there are two main approaches for realizing slow light on-chip, namely the use of coupled resonator optical waveguides (CROWs) and the use of photonic crystal waveguides (PhCWs). Although they have always been considered as quite separate and unrelated structures, from a purely circuit point of view, they both exploit artificial resonances to inhibit optical propagation in forbidden stop bands, the main difference being that PhCWs use

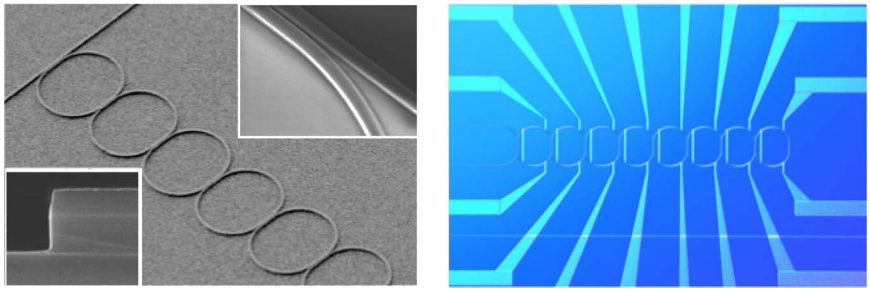

Fig. 1. Ring-based CROW on SOI platform. (Left) Cover layer and heaters not yet deposited. The two insets show the waveguide cross section and a directional coupler. (Right) Top view of an 8-ring CROW with heaters.

optical cavities with a typical length on the order of half a wavelength, while CROWs are typically made of cavities that range in size from a few tens to some thousands of wavelengths. This geometric difference in size implies a fundamental difference in the slow-light bandwidth that can be achieved so that applications so far have been at noncomparable bit rates. Continuously tunable delay lines have been successfully demonstrated in CROWs fabricated in glass ring resonators (RRs) operating at data rates from a few gigabits per second up to 25 Gb/s [2]–[4]. Much shorter pulses ($<$ 10 ps) are typically considered in the case of PhCWs, where state-of-the-art results include tunable delays of up to 74 ps using 3.4-ps-long pulses, corresponding to a tunable capacity of 22 bits [5].

In fact, the absence of a systematic comparison between PhCWs and CROWs is not only due to the intrinsic nature of the two structures but also depends on a cultural background issue: people involved in PhCWs often do not deal with CROWs and *vice versa.* Due to the different nature of the reported applications, attempts to compare the two structures have been limited to the indirect evaluation of suitably normalized figures of merit, such as the delay-bandwidth product, the fractional delay (i.e., the maximum achievable delay in bit units), and the fractional loss per delayed bit.

In this work we report what is, to the best of our knowledge, the first direct comparison between CROWs and PhCWs for the same slow-light application. In the spirit of a fair comparison, the two structures were fabricated on the same silicon-on-insulator (SOI) technological platform, with the same fabrication facilities and evaluated under the same signal bit-rate conditions. We compare the frequency- and time-domain response of the two different structures, the physical mechanism underlying the tuning of the delay, the main limits induced by loss and dispersion, and the impact of CROWs and PhCWs tunable delay lines on the transmission of data streams intensity and phase modulated up to 100 Gb/s.

The paper is organized as follows. The fabrication technology used for the fabrication of CROWs and PhCWs is described in Section 2. Sections 3 and 4 are devoted to descriptions of the working principles, the characterization and the transmission performance of the two structures. As an example of application, Section 5 explains how CROWs and PhCWs can be exploited for achieving pulse synchronization in a 100-Gb/s system. Finally, a discussion comparing the main similarities and differences between the performances of CROWs and PhCWs is reported in Section 6.

2. Structures and Technology

Scanning electron microscope pictures of the two structures considered in this paper are shown in Figs. 1 and 2. Both devices were fabricated on a SOITEC SOI wafer consisting of a 220-nm-thick silicon guiding layer on a 2-μm-thick layer of buried oxide and the device patterns were defined using a VISTEC VB6 UH EWF electron beam lithography machine. The fabrication were carried out at the James Watt Nanofabrication Centre of the University of Glasgow according to designs developed by the Policom-DEI group at Politecnico di Milano (for the RR-based CROWs) and by the Photonic Crystals Research group at St. Andrews University (for PhCWs). A detailed

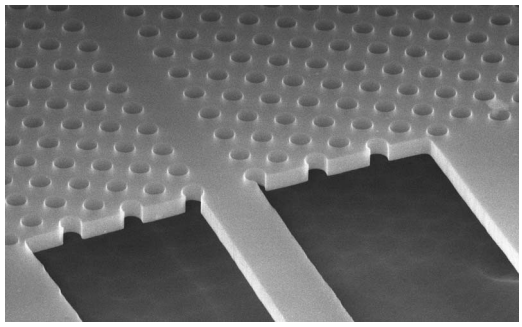

Fig. 2. Silicon membrane PhCW.

description of the technological processes can be found in [6] and [7] for the CROW and the PhC structures, respectively.

2.1. Silicon CROWs

The fabricated CROWs consist of a number (ranging from six to 20) of identical racetrack RRs with a radius of 20 μm and a 16-μm-long straight coupling section. The coupling coefficients between RRs are optimized by changing the gap size according to the design technique proposed in [9]. The silicon photonic wire waveguide of both the bus lines and the RRs is 480 nm wide and is buried under a 900-nm-thick silicon oxide layer.

We employed an optimized HSQ electron-beam-resist (hydrogen silsesquioxane (HSQ), commercially supplied as Fox 16, diluted to 50% in a methyl isobutyl ketone MIBK) solution. The pattern was generated by e-beam lithography with proximity correction and stitching compensation to achieve low propagation losses, typically ranging from 1 to 3 dB/cm [6] and an accuracy better than 0.5 nm on the waveguide dimensions. An upper cladding layer of silica was then used to embed the entire structure and ensure better mechanical resistance—and further protection from subsequent chemical processes. An optimum thickness for the buffer layer of a total of 900 nm (520 nm of HSQ spin-on glass, plus 480 nm of deposited silica) was used, in order to guarantee efficient heat transfer and, at the same time, a negligible contribution to optical propagation losses.

A metallic heater structure consisting of a 50-nm-thick highly resistive layer of nichrome (NiCr) was deposited on each RR and connected via low-resistance gold electrodes. The NiCr layer was patterned using lift-off to obtain 0.9-μm-wide stripes. The heaters were placed only over the bent waveguide sections of the RRs to avoid direct heating of the directional couplers and to reduce the thermal crosstalk between RRs. The heaters resistance was approximately 1.8 kΩ, while the series resistance of the 1-mm-long NiCr/Au contact pad was less than 20 Ω.

The choice of the dimensions of the RRs was the result of a careful compromise between a variety of parameters, such as bandwidth, delay and pulse distortion, bending-induced losses, roughness-induced backscattering, electrical power needed for the tuning of the device, sensitivity to technological tolerances, overall footprint and minimum number of RRs to be tuned. The free spectral range is FSR $=$ 440 GHz, and the power coupling coefficients K_i between the $(i-1)$th and the ith RR are designed to obtain an almost flat-top passband, ranging from 27 to 125 GHz, which is independent of the number of rings [9]. The results presented in the following sections were taken on a CROW with bandwidth $B = 89$ GHz, having $K_1 = 0.79$, $K_2 = 0.33$, $K_3 = 0.18$, $K_4 = 0.16$, and $K_i = 0.15$ for $i \geq 5$. The accuracy of the fabrication process guaranteed proper alignment of the RR resonances with no need for active tuning of the structure.

2.2. Silicon PhCWs

The PhCWs were defined in a suspended membrane, with the air bridge created by using a hydro-fluoric acid wet etch to selectively remove the buried silicon oxide layer. The transitions between the input standard photonic wire waveguide and the PhCW include suitable light injectors as described in [7], [10], and [11], reducing the coupling backreflection below -15 dB (3%) and

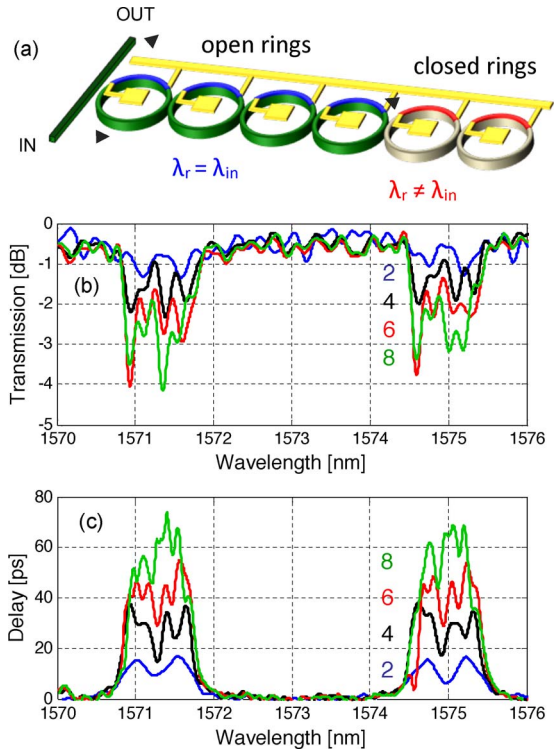

Fig. 3. (a) Sketch of the reflective tunable CROW delay line. Each heater on the rings can be addressed individually. (b) Measured spectral intensity. (c) Group delay characteristic of the CROW. The number of open rings is shown.

ensuring a coupling efficiency higher than 90%. The injectors consist of a fast-light PhCW section followed by a transition to the slow-light PhCW. The difference between the two sections is very subtle, as the lattice constant is changed progressively by only 10–20 nm in the propagation direction [14].

The group index of the transverse electric (TE) mode of the PhCW was engineered by shifting the two innermost rows of holes adjacent to the line defect waveguide (lattice constant $a = 410$ nm, hole radius $r = 0.286a$) by -50 nm and $+10$ nm, respectively, in the transverse direction. This type of waveguide is referred to as dispersion engineered and a detailed description of the principles can be found in [7]. Such a design induces a spectral region that is between 1520 nm and 1560 nm, where the group index smoothly increases as a function of wavelength, followed by a slow-light region above a wavelength of 1560 nm with a nearly constant TE group index of $n_g = 40$. Further details are discussed in Section 4.

The PhC pattern was defined in ZEP-520A electron beam resist using the VISTEC VB6 electron beam writer with a 1.2-mm writing field (thereby reducing the effects of stitching errors on the PhCWs) operating at 100 kV. The pattern was transferred into the silicon layer using reactive ion etching (RIE) with a combination of SF6 and CHF_3 gas. The fabrication process was based on that of [8] and is known to yield world-class low-loss PhC slab waveguides.

3. Tunable Delays in RR-Based CROWs

In an RR-based CROW a continuously tunable delay can be achieved in a simple and effective way by acting on the resonant frequency of each single RR, as schematically shown in Fig. 3(a) [2], [4]. The incoming signal at wavelength λ_{in} couples to the CROW and propagates inside the (open) RRs resonating at $\lambda_r = \lambda_{in}$ until it is reflected by the first off-resonance (closed) RR. Once back to the first RR, the signal couples to the bus waveguide and exits from the output port after an

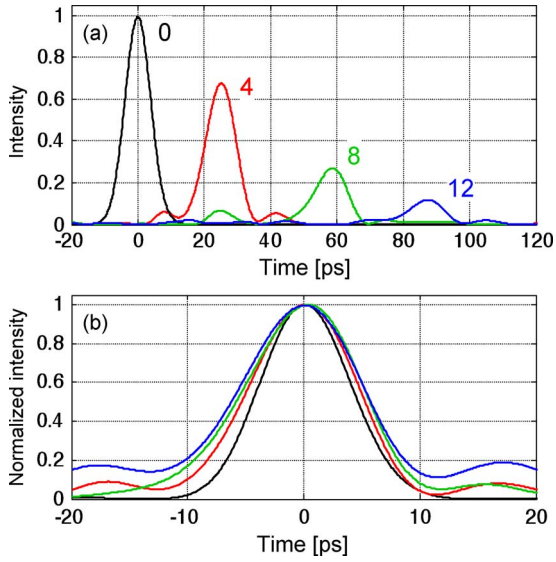

Fig. 4. (a) Delays of a 9-ps Gaussian pulse after propagation through four, eight, and 12 RRs of the CROW.

accumulated delay that can be varied continuously [3]. This type of delay line geometry is said to be reflective or folded.

The tuning technique exploits the thermo-optic effect and requires that the temperature of each RR is individually adjustable. The electric power consumption required to shift the resonance of a silicon RR by half of an FSR is about $P_\pi = 12$ mW, but typically, a smaller spectral shift, roughly equal to twice the bandwidth, is sufficient to change the RR state from open to closed. Note that power consumption scales inversely with the RR finesse $F = \mathrm{FSR}/B$ according to the relation $2P_\pi/F$; this means that, for a given bandwidth, small RRs with a large FSR require less power to be tuned. However, a large value of F also implies also a higher sensitivity to structural imperfections and disorder [12], nonlinearities (the field in the cavity scales linearly with F), and backscattering effects [13]. In our experience, moderate F values between 4 and 10 provide a good tradeoff between power consumption and undesirable side effects. The response time of the thermo-optic effect in these waveguides is around 10 μs, and the thermal crosstalk between adjacent RRs is negligible, despite the small diameter used. This is a clear advantage with respect to glass-based technologies [2].

Fig. 3(b) shows the measured transmission spectrum of the silicon CROW when 2, 4, 6 and 8 RRs are tuned to resonance and Fig. 3(c) shows the corresponding group delay. The input light had a TE polarization state. The in-band ripple was due to nonoptimal impedance matching between the bus line and the CROW and to residual structural disorder along the CROW, i.e., to nonidealities in the coupling coefficients between RRs and drift in the resonance frequencies, as discussed in detail in [12]. The spectral characteristic of Fig. 3(b) has a twofold impact on the time-domain shape of pulses propagating through the structure: the limited bandwidth can induce pulse distortion and broadening, while ripples in the spectral response are associated with echoes and long-scale smooth oscillations. Both these effects result in intersymbol interference (ISI) when a data stream is delayed by the CROW: an effect that is analysed in more detail in the remainder of this section and in Section 6.

The 89-GHz-wide transmission band of the CROW can accommodate Gaussian pulses with a full-width half-maximum (FWHM) time width as short as 9 ps, which are suitable for a 100-Gb/s on-off keying (OOK) transmission system. The input pulse and the delayed output pulses are shown in Fig. 4(a) and, superimposed after unitary peak normalization, in Fig. 4(b) for a direct envelope comparison. At resonance, the group index of the RRs is $n_g = 2\pi c/BL_r = 14.3$, where $2\pi/B = 7.5$ ps [3] is the double-transit delay per RR. A suitable detuning of the last open RR allows for a fine control of the delay with a fraction of picosecond resolution [3]. By using 12 open RRs, we have achieved a

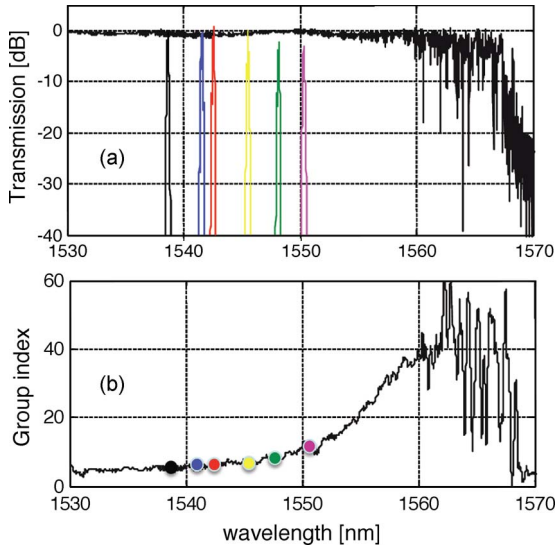

Fig. 5. (a) Measured transmission spectrum of a 4-mm-long dispersion-engineered PhCW (see text for waveguide dimensions). Signal spectra tuned at wavelengths corresponding to different delays are shown. (b) Group delay characteristic of the TE mode.

maximum delay of 89 ps, corresponding to a tunable storage capacity of more than 1 byte and a fractional delay of 0.82 bit/RR. The fractional loss is 0.6 dB/bit and the delayed pulses undergo acceptable broadening (around 20%) and moderate level of ISI. After four delayed bits, the peak intensity decreases further than expected from propagation losses due to the broadening induced by chromatic dispersion. After an 8-bit delay the pulse FWHM was less than 11 ps and the extinction ratio was reduced to 7 dB, which is still acceptable for low-penalty transmission.

Two considerations concerning pulse distortion and loss are worth to be mentioned. Envelope distortions are mainly due to the limited bandwidth of the CROW with respect to the signal bandwidth; therefore, longer pulses with a narrower spectrum experience less distortion, yet with a fractional delay that is reduced accordingly. Regarding loss, assuming, conservatively, 2.5 dB/cm for the waveguide attenuation and a group index value of $n_g = 4.2$, the fractional loss theoretical limit [3] is $L_f = \alpha c/B_p n_g = 0.16$ dB/bit [4], where B_p is the pulse bandwidth. This value is significantly lower than the 0.6-dB/bit fractional loss observed in the experimental CROW. The additional loss comes from the excess loss of the directional couplers, estimated about 0.06 dB/coupler, increasing the ring round trip attenuation from 0.04 to 0.16 dB. The filling of the directional couplers gap is thus a critical technological issue deserving special care.

All the results described above were achieved using TE input polarization. However, the transverse magnetic (TM) mode is also efficiently guided by the photonic wire waveguides, even though with a significantly lower effective index due to the weaker confinement in the waveguide. This polarization sensitivity affects both the coupling coefficient and the resonant frequencies of the RRs in such a way that the TM spectral response of the CROW is substantially different from the TE one. Although polarization sensitivity is considered to be a strong limitation for many applications, it could also be effectively exploited. For instance, in previous contributions we demonstrated that, if the TE and TM passbands of the CROW do not overlap, a differential delay between the two polarization states can be originated and accurately controlled [15]. This unique property is exploited in Section 5 to operate on polarization multiplexed signals.

4. Tunable Delays in Photonic Crystals

The technique employed for tuning the delay in RR-based CROWs cannot readily be employed in silicon PhCWs, where the single "cascaded cavities" correspond to the $\lambda/2$-scale unit cells of the lattice and are too small to be accessed and tuned individually. However, different delays can be

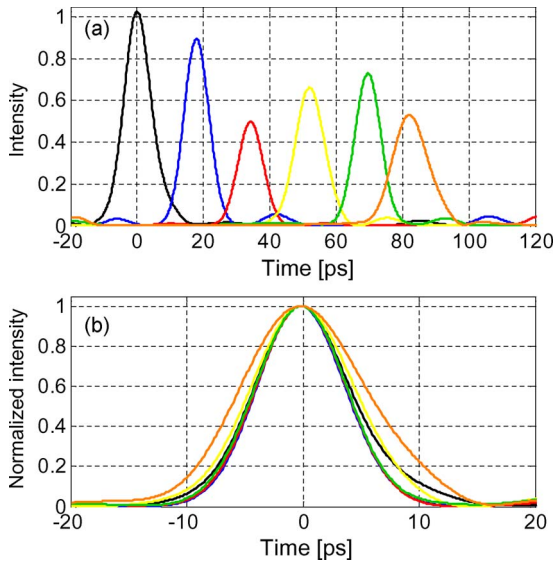

Fig. 6. (a) Delay of a single 9-ps Gaussian pulse achieved by tuning the signal wavelength at 1538.5 nm (black), 1541.5 nm (blue), 1542.5 nm (red), 1545.5 nm (yellow), 1548 nm (green), and 1550.5 nm (purple). The total delay is more than 1 byte or 83 ps. (b) Same but pulses are normalized and overlapped.

obtained by exploiting the wavelength-dependent group delay characteristic that, in the case of TE polarization, increases smoothly approaching the band edge, as shown in Fig. 5, where the transmission and group delay of a fabricated 4-mm-long PhCW are shown. The spectral oscillations are due to imperfections of the PhC structure [21], but the impact on signal distortion can be acceptable up to a group index of $n_g = 40$, as shown in the following.

In the spectral region from 1535 nm to 1550 nm, the TE group index increases almost linearly with a slope $dn_g/d\lambda = 0.45\ \text{nm}^{-1}$ that, for a 4-mm-long waveguide, corresponds to a time delay slope of 6 ps/nm, i.e., to a chromatic dispersion of $1.5\ \text{ps}/(\text{nm} \cdot \text{mm})$. This dispersion value results in a dispersion length [22] $L_D = 15.4$ mm for a 9-ps FWHM Gaussian pulse, thus implying that in this wavelength range the 4-mm-long PhC operates in an almost dispersion-free regime at bit rates up to 100 Gb/s. As a comparison, note that the same group delay dispersion is induced by a 350-m-long standard single mode optical fiber for which the chromatic dispersion is 17 ps/(nm km).

The wavelength dependence of the PhCW group index was exploited to delay 9-ps FWHM Gaussian pulses. Delay tunability was demonstrated by shifting the pulse carrier to different wavelengths in the range from 1537 to 1551 nm. In Fig. 5(a), the measured signal spectra are superimposed onto the PhCW transmission and marked with circles onto the group delay characteristic in Fig. 5(b). In the wavelength range under consideration the delay changes continuously by 82 ps, resulting in more than 1 byte of delay at 100 Gb/s. The input pulse and the delayed output pulses are shown in Fig. 6(a) and superimposed after peak intensity normalization in Fig. 6(b) for a direct comparison. Since the PhCW operates well below L_D, pulse broadening is less than 2 ps in the worst case, a value that is tolerable in most transmission systems. The intensity fluctuations at different delays are related to the aforementioned spectral ripple of the PhCW transfer function and the average insertion loss is about 0.35 dB/bit at 100 Gb/s, that is about 35 dB/ns. Above 1550 nm, up to 1560 nm, chromatic dispersion increases rapidly, and the maximum manageable bit rate decreases accordingly: In this spectral range, where L_D drops to 2.5 mm at 100 Gb/s, signals at bit rates below 40 Gb/s $(L_D = 18\ \text{mm})$ can sustain large tunable delays with acceptable pulse broadening. Note, however, that at lower bit rates the absolute delay per bit increases, as well as the fractional loss.

The TM-polarized mode is guided in the PhCW by total internal reflection and propagates with negligible loss and with an almost wavelength-independent group index. Further optimization could

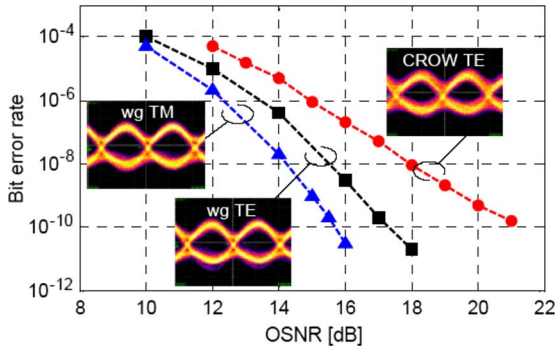

Fig. 7. BER measurements after propagation through 1-cm-long silicon nanowire (both TE and TM polarization, CROW in locked state) and through the CROW (TE only) tuned to induce 20-ps delay.

also be possible through engineering the dispersion of the TM mode. As in the case of RR-based CROWs, the different propagation regime of the two polarizations can be exploited to introduce a controllable differential delay between two data streams encoded on orthogonal polarization states, as explained in the next section.

5. Pulse Synchronization in PolDM-DQPSK Format

The different spectral behavior of TE and TM modes is a feature that could find useful applications in polarization-division multiplexing (PolDM) transmission systems, where the management of the mutual delay between two orthogonally polarized data channels transmitted on the same fiber is a crucial requirement to optimize system performance [16], [17].

Here, we show the synchronization of two 50-Gb/s differential quadrature phase-shift keying (DQPSK)-modulated signals encoded on orthogonal polarization states as one of the most advanced demonstration of the potential of our silicon devices. The two data streams were independently generated, multiplexed by using a polarization beam combiner, and coupled to the TE and TM modes, respectively, of the silicon bus waveguide in order to arrive at the CROW or PhCW input time overlapped (with 0 ps of relative delay) and with the same optical power. At the end facets of the chip, the waveguide was directly coupled with a lensed fiber with no on-chip mode adaptor. Transmission performance was evaluated by means of bit-error-rate (BER) measurements on two orthogonally polarized channels with a $2^7 - 1$ pseudorandom bit sequence (PRBS) in a system test bed [18], [19]. After propagation in the device, TE- and TM-polarized signals where polarization demultiplexed and each one was detected by a pair of integrated unbalanced Mach–Zehnder interferometers [20] to recover the DQPSK symbol constellation.

Concerning the CROW, the TE-polarized channel is aligned with the TE CROW passband and arbitrarily delayed with respect to the TM-polarized channel that travels only in the bus waveguide [15]. The 30-GHz-wide spectrum of the TE-encoded stream of the 100-Gb/s signal is entirely contained within the passband and experiences a negligible distortion. Back-to-back BER curves are reported in Fig. 7 for both polarizations with pulses in time-overlapped (0-ps delay, CROW in locked state) and time-interleaved mode (20-ps delay, TE propagating through to the CROW) conditions, the latter given by propagation through less than 3 RRs. Error-free propagation $(\mathrm{BER} < 10^{-9})$ in the CROW is achieved with a 3-dB optical signal-to-noise ratio (OSNR, measured over 0.5 nm) penalty with respect to propagation in the straight waveguide only, demonstrating the low impact of the device on the signal integrity. The performance of the orthogonal TM-polarized channel, which was not coupled into the CROW and propagated only along the 1-cm-long bus line, was not affected by the CROW condition. Note that the TE-polarized channel with the CROW in locked state (null delay) exhibited about 1-dB OSNR penalty with respect to the TM-polarized one. This was due to the cavity effect originating from the facet reflections, which are much stronger for TE polarization (30% TE reflectivity, 10% TM reflectivity) and generate spurious ISI effects in the eye diagram, as shown in the insets of Fig. 7.

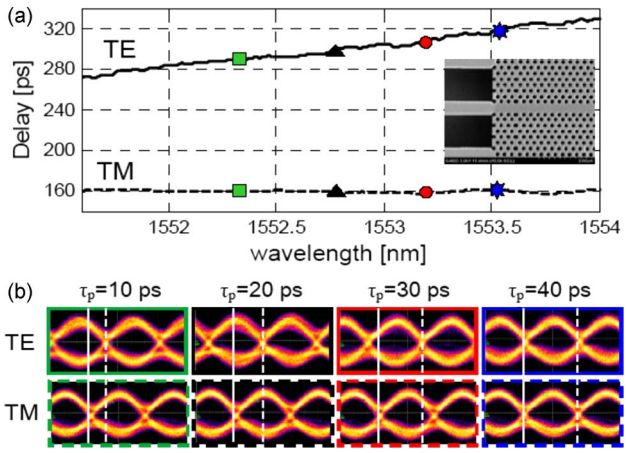

Fig. 8. (a) Group delay induced by the 4-mm-long PhCW for both TE and TM modes at different wavelengths. (b) Eye diagrams of the 100-Gb/s RZ-PolDM-DQPSK signals (TE and TM polarizations) propagating through at the points marked in (a).

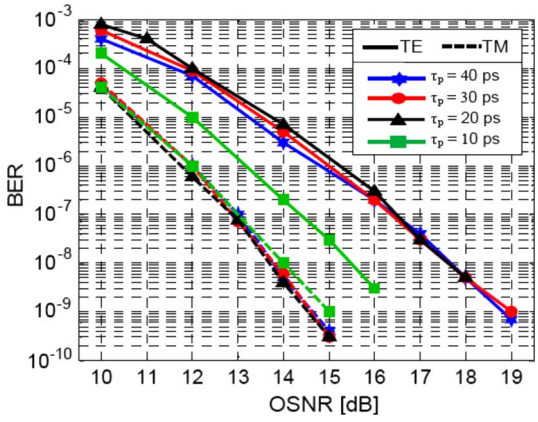

Fig. 9. BER measurements after propagation through the PhCW for different mutual delays τ_p between TE and TM polarization.

Fig. 8(a) shows the measured group delay of the 4-mm-long PhCW for both TE and TM polarization. The group delay for the TE polarization increases by 40 ps in the region between 1552.35 nm and 1553.5 nm, while the group delay for the TM mode is flat. Such a polarization selectivity was exploited to introduce a mutual delay τ_p between the two orthogonally polarized channels of the 100-Gb/s PolDM-DQPSK data stream. Transmission performance was evaluated by using the same system test bed employed for the characterization of the RR-based silicon CROW. To control the differential delay, the spectrum of the PhC was thermo-optically shifted with respect to the signal carrier (1552.35 nm). Fig. 8(b) shows the eye diagrams of the TE- and TM-polarized signals at the output of the PhC at different relative delays. As the PhC spectrum is shifted toward shorter wavelengths, the TE delay is increased by 30 ps (cooling the sample from 48 °C to 15 °C, i.e., 1.2-nm wavelength shift), whereas the TM polarization is insensitive to any thermal change. The temperature stability of the delay is 1 ps/°C, suggesting that subpicosecond accuracy can be easily achieved by means of conventional thermo-cooling systems.

Back-to-back BER curves are shown in Fig. 9 for both polarizations and for different sample temperatures of the sample. The delayed TE channel exhibits a maximum OSNR penalty of 4 dB with respect to the nondelayed TM channel. The better performance of the TE polarization when $\tau_p = 10$ ps (squares) is obtained because the PhC is working in a region with lower n_g, where the device response is less sensitive to fabrication imperfections if compared with higher n_g regions. At

higher n_g, no evident performance degradation is visible for τ_p between 20 and 40 ps. As observed in the case of the RR-based CROW, the performance of TM polarization is insensitive to the thermal tuning of the structure and is better than that of TE polarization because of the reduced cavity effects originating from the facet reflections.

6. Comparison and Discussion

Although RR-based CROWs and PhCWs have always been considered to be quite different structures, we have now demonstrated that some applications could exist where the two domains intersect. In particular, our results show that silicon CROWs and PhCWs can both operate in modern high-capacity transmission systems operating at 100-Gb/s data rate, where they can be used as variable delay lines and data channel synchronizers, while preserving the quality of the transmitted signals.

On the basis of the results reported in Sections 3 and 4, a direct comparison of the main parameters of the two structures will now be presented here, with the aim of pointing out the main limits and advantages of the two different approaches. The discussion does not review the electromagnetic mechanisms of optical propagation in the two structures but rather focuses on their practical exploitation in slow-light applications.

6.1.1. Slowdown factor

CROWs and PhCWs can both operate as "slow-wave structures" and with respect to bare waveguides or optical fibers they generally allow a substantial footprint reduction. The unitary time delay induced by every resonator is simply S/FSR, that is S times the cavity roundtrip time. In CROWs, where the FSR is on the order of tens or hundreds of gigahertz, the unitary delay can be very large, i.e., on the order of several picoseconds, whereas in PhCWs, where the cavity length is typically a fraction of a wavelength, it is on the order of tens of femtosecond only. In the first case an optical pulse is localized in a very few RRs (1.2 RRs in the example of Fig. 4), allowing an easy tuning of the structure, whereas in PhCWs the same pulse spreads over hundreds of lattice periods, even in the slow-light regime. Assuming $n_g = 40$ as the maximum exploitable group index (as discussed later on in this section), the delay provided by the unitary 410-nm-long lattice period is about 55 fs, which implies that a 9-ps pulse spreads over 164 periods and a 40-ps pulse over more than 730 periods.

In both structures, the slowdown factor S is independent of the dimension and type of the cavities. In the CROW considered in Section 3, the slowdown factor is $S = 2\ \mathrm{FSR}/(\pi B) = 2.9$ [23], as well as in the range 2 to 10 for the PhCW (defined as the PhC group index divided by the group index of the silicon slab) in the wavelength region used to achieve a tunable delay for the 100-Gb/s signal. In practical applications, the maximum S that can be used in silicon CROWs is limited to a few tens $(S < 20)$, in order to avoid impairments due to strong sensitivity to disorder [12], nonlinearities, and contradirectional coupling due to backscattering effects [13]. Similar limits exist in PhCWs, preventing the full exploitation of the PhCWs spectral characteristic at wavelengths close to the band edge (i.e above 1560 nm in Fig. 5). In the 4-mm-long PhCW of Section 4, chromatic dispersion sets the ultimate limit for the transmission of 9-ps pulses, which can propagate in dispersion-free mode up to $S = 4$. Note that this value is surprisingly close to that provided by the RR-CROW of Section 3.

6.1.2. Fractional loss

When used as delay lines, the key figure of merit in both structures is not the loss per unit length but the fractional loss per bit L_f, as defined in Section 3. Note that L_f depends neither on the device dimensions and type, nor on S. The guiding structure with the lowest value of the ratio α/n_g should be preferred, where $\alpha/n_g = 0.6$ dB/cm in the silicon waveguide (with $\alpha = 2.5$ dB/cm and $n_g = 4.2$) and $\alpha/n_g = 1$ dB/cm in the PhCW in the fast-light regime (with $\alpha \simeq 6$ dB/cm and $n_g \simeq 6$), i.e., below a wavelength of 1540 nm. On the basis of this argument, silicon CROWs should outperform silicon PhCWs, but this is not the case in the measurements reported in Figs. 4 and 6, where L_f is 0.6

and 0.35, respectively. The reason for this apparent discrepancy is that the n_g and α values to be considered when evaluating the fractional loss are affected by all the single elements of the slow-light structure and not only by the group index and attenuation of the bare waveguide. As discussed in Section 3, in CROWs the directional coupler excess loss α_c dominates the RR roundtrip loss, and hence L_f. The effect of α_c can be taken into account by defining an effective propagation loss for the RRs as $\alpha_{CROW} = \alpha + 2\alpha_c/L_r = 10$ dB/cm, where L_r is the RR's length. To reduce the impact of α_c for a given delay, it is convenient to use large RRs with a small finesse (i.e., a low S), rather than small RRs with a high S. In PhCWs, below a group index value of approximately 40, the loss scales approximately linearly with n_g [24]. This dependence makes the fractional loss L_f of the PhCWs measured in Section 4 almost independent of n_g all over the entire wavelength range under consideration, i.e., up to a wavelength of 1560 nm. Above this wavelength, backscattering induced by structural disorder dominates and causes the strong oscillations in the spectral response of Fig. 5. However, disorder effects can be observed also below 1560 nm since it is responsible for the peak power fluctuations observed in Fig. 6: for instance, the lower intensity of the pulse delayed by 35 ps is not due to out-of-plane loss enhancement mechanisms but is due to a partial reflection occurring somewhere along the PhCW at the wavelength of 1542 nm.

6.1.3. Thermal tuning

In theory, the required control of the delay can be accomplished in both CROWs and PhCWs by using thermal activation. Yet, owing to the different working principle of the two structures, substantial differences arise. In a CROW, provided that fabrication accuracy guarantees that all the RRs resonate at the same wavelength, only two RRs must be activated to control continuously the delay from 0 to the maximum achievable delay [4]. In this condition, the maximum temperature change needed in the RRs is 40 °C (corresponding to a $2B$ frequency shift), and from the relations given in Section 3, the maximum power consumption is around 19 mW independent of the desired delay. In a disordered CROW, all the RRs have to be tuned to compensate for the resonance spreading caused by fabrication inaccuracies. In case of high finesses or disordered CROWs, most of the power consumption arises from the realignment of the RRs' resonances. For example, in the worst case in which the RR resonances are uniformly spaced within a FSR, the average power consumption required to realign N RRs is $(\mathrm{N}-1)P_\pi$, yielding a total consumption of 132 mW in a CROW with 12 RRs.

In PhCWs, the group delay can be increased by cooling the whole structure. Below a wavelength of 1550 nm, where the average slope is only 0.15 ps/°C, delays above a few tens of ps are not practically achievable by using conventional thermoheaters. Above 1550 nm, the delay versus temperature slope increases to 1 ps/°C, thus enabling the control of the delay over a range exceeding a 100 ps. Photonic crystals may also be encased in oxide to employ a similar thermal heating scheme to that used to tune the CROWs in Section 3 [25]. This does impose some additional design restrictions (the need to operate below the silica light line) which tends to reduce the maximum group index possible, though on the basis of [26], the loss/unit time is not expected to increase. However, the complete device area must be heated, resulting in a larger power consumption with respect to CROWs. Additionally, this power consumption will be proportional to the delay required. In principle, the group delay spectral dependence can be exploited recurring to a wavelength conversion scheme as proposed in [27], [28], rather than to thermal activation. In comparison to dispersive fibers, the strong chromatic dispersion provided by PhCWs could provide tunable delays with an extremely small footprint.

6.1.4. Structural disorder

A further consideration concerns the sensitivity of CROWs and PhCWs to fabrication imperfections. For a given slowdown S, the relative tolerance on the value of the coupling elements (directional couplers in CROWs and holes in PhCWs, respectively) and on cavity resonant frequency is the same for both structures. This consideration must be translated into

requirements on the tolerances of the physical dimensions of the coupling element, on the cavity length, and on the uniformity of the layer refractive index, which is a quite difficult task. However, it appears to be evident that the control over the total cavity length is easier to achieve in PhCWs rather than in RRs, which often require alignment of the resonances by individual tuning of each resonator. Against this, PhCWs periods cannot readily be realigned individually, thus preventing their exploitation at $n_g > 40$, that is $S > 10$ [29]. Not surprisingly, RR-CROWs with $S > 10$ often require realignment of the resonances to achieve good performance.

6.1.5. Transmission quality performance

Pulse propagation in CROWs and PhCWs is subject to several different sources of degradation. In CROWs (see the comments to Fig. 7), nonidealities in the coupling coefficients and misalignments in the resonant frequencies of the cavities generate a distributed crosstalk between the pulses, resulting in ISI effects. In PhCWs, the aforementioned pulse intensity fluctuations which are visible in Fig. 6, are related to frequency-domain ripples induced by lattice imperfections, whereas pulse broadening is associated with chromatic dispersion. Besides evaluating the envelope distortion of wideband signals, our measurements demonstrate that slow-light propagation in CROWs and PhCWs preserves encoded information in the phase of the propagating signals. The two structures show error-free propagation with a comparable OSNR penalty after 20-ps delay when used to adjust the time interleaving between the two data channels of a 100-Gb/s PolDM-DQPSK signal.

6.1.6. Footprint

As a final remark, it is interesting to note that the footprint of the silicon CROW $(480 \times 56\ \mu\text{m}^2)$ and that of the PhCW $(4000 \times 6\ \mu\text{m}^2)$ employed to realize 8-bit capacity tunable delay lines at the same bit rate of 100 Gb/s are quite similar: $\simeq 0.025\ \text{mm}^2$. The length of the PhCW depends on the maximum n_g change that can be achieved without pulse distortion, i.e., from $n_g = 6$ (at 1537 nm) to $n_g = 12.5$ (at 1551 nm). This limit sets the minimum length of the structure, resulting in a 4-mm-long PhCWs to control the delay over 80 ps. Note that smaller structures providing the same delay could be realized, but at the expense of a higher factor S (or equivalently of a higher n_g), that would cause higher sensitivity to disorder and nonidealities, higher attenuation, and more critical delay management.

7. Conclusion

Tunable delay lines in CROWs and PhCWs geometries were fabricated in the same silicon process line and compared with the same wideband signals. The results presented are, to the best of our knowledge, the first demonstration of slow-light silicon photonics in the context of the emerging 100-Gb/s optical communication systems and one of the first comparison between RRs and PhCWs. Despite well-known fundamental differences in the physics and in the management of the two structures, the main result of this study is that, in the considered domain of applications, CROWs and PhCWs exhibit much more similar behavior than one might otherwise expect.

Both structures were used to realize a 100-Gb/s continuously tunable delay line with 1-byte capacity, moderate fractional loss (< 0.6 dB/bit) and acceptable pulse broadening ($< 20\%$). The main advantage of CROWs is the possibility of tuning each resonator independently, thus enabling a more flexible and power efficient tuning of the delay, as well as full reconfiguration of the structure. On the other hand, our PhCWs show a somewhat better fractional loss (i.e., lower loss) and lower pulse shape distortion, at least in the fast-light regime. In the slow-light regime $(n_g > 15)$, where PhCWs can get larger delays, disorder effects and chromatic dispersion progressively degrade transmission performances.

When phase modulated signals propagate through CROWs and PhCWs, a variable delay can be introduced without corrupting phase information. System measurements show that both structures can be used to synchronize the two orthogonally polarized data streams of a 100-Gb/s

PolDM-DQPSK system with a similar OSNR penalty of less than 4 dB when the mutual delay is changed over 20 ps.

The similar performance observed in our experiments depends on the fact that data rates from 100 Gb/s to several hundreds of gigabits per second are the intersection zone where CROWs and PhCWs can be placed in direct competition. Lower data rates, where longer absolute delays are required and propagation loss becomes a critical issue, are the preferred domain of CROWs fabricated with large RRs in low-loss technology, for instance, high-index-contrast glasses. At data rates in the terabit range, requiring bandwidths that are unsuitable for RR-based architectures, PhCWs probably remain the leading technology.

Acknowledgment

The authors acknowledge the whole team of the James Watt Nanofabrication Centre of the University of Glasgow for the support in fabricating the devices and R. Siano and M. Ferrario for the BER measurements on the PoliCom 100-Gb/s system test bed.

References

[1] R. S. Tucker, P.-C. Ku, and C. J. Chang-Hasnain, "Slow-light optical buffers: Capabilities and fundamental limitations," *J. Lightw. Technol.*, vol. 23, no. 12, pp. 4046–4066, Dec. 2005.

[2] F. Morichetti, A. Melloni, A. Breda, A. Canciamilla, C. Ferrari, and M. Martinelli, "A reconfigurable architecture for continuously variable optical slow-wave delay lines," *Opt. Exp.*, vol. 15, no. 25, pp. 17 273–17 282, Dec. 2007.

[3] F. Morichetti, A. Melloni, C. Ferrari, and M. Martinelli, "Error-free continuously-tunable delay at 10 Gbit/s in a reconfigurable on-chip delay-line," *Opt. Exp.*, vol. 16, no. 12, pp. 8395–8405, Jun. 2008.

[4] A. Melloni, F. Morichetti, C. Ferrari, and M. Martinelli, "Continuously tunable 1-byte delay in coupled-resonator optical waveguides," *Opt. Lett.*, vol. 33, no. 20, pp. 2389–2391, Oct. 2008.

[5] J. Adachi, N. Ishikura, H. Sasaki, and T. Baba, "Wide range tuning of slow light pulse in SOI photonic crystal coupled waveguide via folded chirping," *IEEE J. Sel. Topics Quantum Electron.*, vol. 16, no. 1, pp. 192–199, Jan./Feb. 2010.

[6] M. Gnan, S. Thorns, D. S. Macintyre, R. M. De La Rue, and M. Sorel, "Fabrication of low-loss photonic wires in silicon-on-insulator using hydrogen silsesquioxane electron-beam resist," *Electron. Lett.*, vol. 44, no. 2, pp. 115–116, Jan. 2008.

[7] J. Li, T. P. White, L. O'Faolain, A. Gomez-Iglesias, and T. F. Krauss, "Systematic design of flat band slow light in photonic crystal waveguides," *Opt. Exp.*, vol. 16, no. 9, pp. 6227–6232, Apr. 2008.

[8] L. O'Faolain, X. Yuan, D. McIntyre, S. Thoms, H. Chong, R. M. De La Rue, and T. F. Krauss, "Low-loss propagation in photonic crystal waveguides," *Electron. Lett.*, vol. 42, no. 25, pp. 1454–1455, Dec. 2006.

[9] A. Melloni and M. Martinelli, "Synthesis of direct-coupled-resonators bandpass filters for WDM systems," *J. Lightw. Technol.*, vol. 20, no. 2, pp. 296–303, Feb. 2002.

[10] J. P. Hugonin, P. Lalanne, T. P. White, and T. F. Krauss, "Coupling into slow-mode photonic crystal waveguides," *Opt. Lett.*, vol. 32, no. 18, pp. 2638–2640, Sep. 2007.

[11] T. P. White, L. C. Botten, C. Martijn de Sterke, K. B. Dossou, and R. C. McPhedran, "Efficient slow light coupling in a photonic crystal waveguide without transition region," *Opt. Lett.*, vol. 33, no. 22, pp. 2644–2646, Nov. 2008.

[12] C. Ferrari, F. Morichetti, and A. Melloni, "Disorder in coupled-resonator optical waveguides," *J. Opt. Soc. Amer. B, Opt. Phys.*, vol. 26, no. 4, pp. 858–866, Apr. 2009.

[13] F. Morichetti, A. Canciamilla, M. Martinelli, A. Samarelli, R. M. De La Rue, M. Sorel, and A. Melloni, "Coherent backscattering on optical microring resonators," *Appl. Phys. Lett.*, vol. 96, no. 081112, 3 p., 2010, doi: 10.1063/1.3330894.

[14] S. A. Schulz *et al.,* "Dispersion free slow light in photonic crystals: A comparison," *J. Opt.,* Feb. 2010, submitted for publication.

[15] C. Ferrari, F. Morichetti, A. Canciamilla, A. Melloni, and M. Martinelli, "Differential polarization delay in coupled-resonator optical waveguides," *IEEE Photon. Technol. Lett.*, vol. 21, no. 20, pp. 1541–1543, Oct. 15, 2009.

[16] C. Wree, N. Hecker-Denschlag, E. Gottwald, P. Krummrich, J. Leibrich, E.-D. Schmidt, B. Lankl, and W. Rosenkranz, "High spectral efficiency 1.6-b/s/Hz transmission (8 $\times$ 40 Gb/s with a 25-GHz grid) over 200-km SSMF using RZ-DQPSK and polarization multiplexing," *IEEE Photon. Technol. Lett.*, vol. 15, no. 9, pp. 1303–1305, Sep. 2003.

[17] J. Renaudier, O. Bertran-Pardo, H. Mardoyan, P. Tran, M. Salsi, G. Charlet, and S. Bigo, "Impact of temporal interleaving of polarization tributaries onto 100-Gb/s coherent transmission systems with RZ pulse carving," *IEEE Photon. Technol. Lett.*, vol. 20, no. 24, pp. 2036–2038, Dec. 2008.

[18] F. Morichetti, C. Ferrari, A. Canciamilla, M. Torregiani, A. Melloni, A. Samarelli, R. De La Rue, and M. Sorel, "Processing light in coupled ring resonators," presented at the Integrated Photonics Nanophotonics Research Applicat. Conf., Honolulu, HI, Jul. 2009, Paper JMA2.

[19] P. Boffi, M. Ferrario, L. Marazzi, P. Martelli, P. Parolari, A. Righetti, R. Siano, and M. Martinelli, "Stable 100-Gb/s POLMUX-DQPSK transmission with automatic polarization stabilization," *IEEE Photon. Technol. Lett.*, vol. 21, no. 11, pp. 745–747, Jun. 2009.

[20] F. Morichetti, R. Costa, G. Cusmai, A. Cabas, M. Fere, M. C. Ubaldi, A. Melloni, and M. Martinelli, "Integrated optical receiver for RZ-DQPSK transmission systems," presented at the Optical Fiber Communication Conf., Los Angeles, CA, 2004, Paper FC8.
[21] L. O'Faolain, T. P. White, D. O'Brien, X. Yuan, M. D. Settle, and T. F. Krauss, "Dependence of extrinsic loss on group velocity in photonic crystal waveguides," *Opt. Exp.*, vol. 15, no. 20, pp. 13 129–13 138, Oct. 2007.
[22] G. P. Agrawal, *Nonlinear Fiber Optics,* 2nd ed. Boston, MA: Academic, 1995.
[23] A. Melloni, F. Morichetti, and M. Martinelli, "Linear and nonlinear pulse propagation in coupled resonator slow-wave optical structures," *Opt. Quantum Electron.*, vol. 35, no. 4/5, pp. 365–379, Mar. 2003.
[24] S. Hughes, L. Ramunno, J. F. Young, and J. E. Sipe, "Extrinsic optical scattering loss in photonic crystals: Role of fabrication disorder and photon group velocity," *Phys. Rev. Lett.*, vol. 94, no. 3, p. 033903, Jan. 2005.
[25] D. M. Beggs, T. P. White, L. Cairns, L. O'Faolain, and T. F. Krauss, "Ultrashort photonic crystal optical switch actuated by a microheater," *IEEE Photon. Technol. Lett.*, vol. 21, no. 1, pp. 24–26, Jan. 2009.
[26] T. P. White, L. O'Faolain, J. Li, L. C. Andreani, and T. F. Krauss, "Silica-embedded silicon photonic crystal waveguides," *Opt. Exp.*, vol. 16, no. 21, pp. 17 076–17 081, Oct. 2008.
[27] E. Myslivets, N. Alic, S. Moro, B. P. P. Kuo, R. M. Jopson, C. J. McKinstrie, M. Karlsson, and S. Radic, "1.56-μs continuously tunable parametric delay line for a 40-Gb/s signal," *Opt. Exp.*, vol. 17, no. 14, pp. 11 958–11 964, Jul. 2009.
[28] S. R. Nuccio, O. F. Yilmaz, S. Khaleghi, X. Wu, L. Christen, I. Fazal, and A. E. Willner, "Tunable 503 ns optical delay of 40 Gbit/s RZ-OOK and RZ-DPSK using a wavelength scheme for phase conjugation to reduce residual dispersion and increase delay," *Opt. Lett.*, vol. 34, no. 12, pp. 1903–1905, Jun. 2009.
[29] L. C. Andreani and D. Gerace, "Light-matter interaction in photonic crystal slabs," *Phys. Stat. Sol. (B)*, vol. 244, no. 10, pp. 3528–3539, Oct. 2007.